

## Dynamically Stabilized Growth of Polar Oxides: The Case of MgO(111)

Vlado K. Lazarov,<sup>1,2,\*</sup> Zhuhua Cai,<sup>3</sup> Kenta Yoshida,<sup>2</sup> K. Honglian L. Zhang,<sup>4</sup> M. Weinert,<sup>5</sup>  
Katherine S. Ziemer,<sup>3</sup> and Philip J. Hasnip<sup>1</sup>

<sup>1</sup>*Department of Physics, University of York, York YO10 5DD, United Kingdom*

<sup>2</sup>*York JEOL Nanocentre, University of York, YO10 5BR, United Kingdom*

<sup>3</sup>*Chemical Engineering Department, Northeastern University, Boston, Massachusetts, 02115, USA*

<sup>4</sup>*Chemistry Department, University of Oxford, Oxford, OX1 3TA, United Kingdom*

<sup>5</sup>*Physics Department, University of Wisconsin-Milwaukee, Milwaukee, Wisconsin, 53211, USA*

(Received 9 April 2011; published 28 July 2011)

By using MgO(111) as a model system for polar oxide film growth, we show by first-principles calculations that H acts as a surfactant, i.e., the H changes its position and bonding during the growth process, remaining in the surface region. Continuous presence of H during the growth of MgO(111) film efficiently removes the microscopic dipole moment, thus enabling the growth of perfect fcc-ordered MgO(111) films. These theoretical predictions are confirmed experimentally by molecular beam epitaxy single crystal growth of MgO(111) on SiC(0001).

DOI: 10.1103/PhysRevLett.107.056101

PACS numbers: 68.43.Bc, 68.35.Ct, 68.37.Og, 68.47.Gh

Intrinsic polar materials, such as metal oxides and compound semiconductors, are some of the most commonly used materials in electronic, magnetic, and chemical applications. It has been recognized for some time that polarity arising from chemical variations at surfaces and interfaces is the main driving force determining the structural and electronic properties [1,2] of nanoscale materials. Along the polar direction, these materials consist of oppositely charged ionic planes; within the so-called electrostatic model, which assumes that each ion keeps its nominal valence charge, such a structural arrangement leads to diverging electric dipole moments with increasing film thickness.

Conceptually, this diverging dipole moment poses fundamental problems in understanding both the structural stability of polar materials (thin films and surfaces) and the observed layer-by-layer growth. Real systems, however, are not composed of fixed charges: the (quantum) electronic degrees of freedom are able to efficiently compensate the surface dipoles, thereby efficiently stabilizing the polar surfaces. Various mechanisms that heal polarity have been reported including surface faceting, surface reconstructions, adatoms, and surface metallization [1–3]. Which mechanism(s) can operate depends on the particular material and how the surface is prepared. It is generally assumed that the growth of strongly ionic polar oxide films (e.g., films with a rock salt structure such as MgO, NiO, CaO, etc.) will be determined by the large surface energies associated with the oxides' (oxygen) vacuum interfaces. Recently, there have been increased efforts to grow MgO along its polar [111] orientation [4–7]. A characteristic of many attempts at layer-by-layer molecular beam epitaxy (MBE) and atomic layer deposition growth is surface roughening, including faceting into neutral surface planes, which appears to be one mechanism for overcoming

polarity [4,8]. For this reason, growth of atomically flat polar oxide films with arbitrary thickness still remains rather challenging.

In order to grow single-crystal polar films of arbitrary thicknesses, mechanisms that heal polarity should be dynamically present during the film growth itself. Surface reconstructions, which require rather high temperatures ( $> 800^\circ\text{C}$ ), and surface faceting into neutral atomic planes are stabilization mechanisms that would prohibit most of the potential technological applications of polar oxide films in device-type heterostructure films. On the other hand, adatoms such as H have been found to heal (quench) the surface dipole moment of some polar oxide surfaces, including MgO(111), very efficiently leaving them in a  $1 \times 1$  termination [9–11]. In this work we show for the example of MgO(111) that H can play the role of surfactant, thus providing a dynamical solution for the polarity constraints throughout the growth of the MgO(111). This property of H can facilitate the defect-free growth of single-crystal MgO(111) films, and potentially open the way for the growth of artificial polar oxide heterostructural superlattices with novel electronic properties. Moreover, the hexagonal symmetry of MgO(111) films in combination with good thermal stability, relatively high dielectric constant, and its spin filtering properties have the potential to enable new complementary metal-oxide-semiconductor (CMOS) and spintronics devices based on wide band gap semiconductors and ferrite oxides.

MgO is a strongly bonded ionic oxide with alternating cationic ( $\text{Mg}^{2+}$ ) and anionic ( $\text{O}^{2-}$ ) atomic planes in the fcc ABC-type stacking along the [111] direction; the nominal electric dipole moment in the repeat unit normal to the surface makes MgO(111) a polar surface. MgO(111) has been widely used as a model system in both theoretical and experimental studies of polar oxide thin films and surfaces.

In addition to various surface reconstructions that stabilize the MgO(111) surface [12,13], the OH termination has been found to be a dominant mechanism for surface stabilization at low temperatures (up to 800 °C) [9,10]. Recently, it has been shown that even the  $(\sqrt{3} \times \sqrt{3})R30^\circ$  reconstruction, that occurs at temperatures above 900 °C, involves H as a topmost layer [13].

To theoretically study the growth of MgO(111) from first-principles, we use both the full-potential linearized augmented plane-wave (FLAPW) method (with an implementation called *flair*) [14,15] and the plane-wave pseudopotential (CASTEP code) [16] approaches in a periodic slab geometry, consisting of 13 atomic layers constructed to have inversion symmetry, i.e., the top and bottom surfaces have the same termination which avoids artificial dipole-dipole interactions between the periodically repeated supercells. The calculated MgO bulk lattice constants for both the local density approximation (LDA) value of 4.194 Å and the generalized gradient approximation value of 4.266 Å are in good agreement with the experimental MgO bulk lattice constant of 4.217 Å; we choose to use LDA in this study because of the slightly better agreement with experiment. The internal atomic positions were fully relaxed (forces  $< 5 \times 10^{-4}$  eV/Å). The FLAPW calculations used a plane-wave basis cutoff of 170 eV and a sampling of the Brillouin zone corresponding to  $\sim 100$   $k$  points in the irreducible zone for bulk MgO. The potential energy surfaces, which required  $\sim 1000$  separate calculations, were determined using CASTEP (LDA ultrasoft pseudopotentials with a 490 eV plane-wave cutoff, a Monkhorst-Pack Brillouin zone sampling density of  $0.04 \times 2 \pi/\text{Å}$ , and a Fermi-level broadening of 0.2 eV). At each step of the potential energy surface calculation, the  $x$  and  $y$  coordinates of the hydrogen were constrained, with all other atoms free to relax until converged to  $10^{-3}$  Å. As a consistency check, several representative structures were calculated using both codes: the optimized structures were identical and formation energies agreed within a few hundredths of an electron volt; in addition, we have verified that the results are essentially unchanged with increases of the number of atomic layers, basis size, and  $k$ -point sampling.

The MgO film was grown by plasma-oxygen-assisted MBE on  $6h - \text{SiC}(0001)$ . The substrate was cleaned in a hydrogen flow furnace. The cleaned  $6h - \text{SiC}(0001)$  surface showed a  $(\sqrt{3} \times \sqrt{3})R30^\circ$  surface reconstruction. The growth temperature was 150 °C. TEM images were acquired on an aberration-corrected JEOL 2200FS transmission electron microscope and cross-sectional TEM specimens were prepared using conventional methods which include mechanical thinning and polishing followed by Ar ion beam milling.

We first consider homoepitaxial growth of MgO. The starting surface is  $1 \times 1$  OH-terminated MgO(111), since all the MgO(111)  $1 \times 1$  experimentally studied surfaces show this surface structure [9,10]. Next we consider

layer-by-layer growth, corresponding to growth by atomic layer deposition (ALD) or MBE. The two crucial steps necessary to understand the growth process on such a surface are (i) the arrival of the “first” Mg atomic layer and then (ii) the subsequent arrival of the second O layer, i.e., a Mg (O) atom on a MgO(111)-OH  $1 \times 1$  cell. Of critical importance is the role of H, structurally and energetically.

Figure 1(a) shows a cross section view along the  $[1, -1, 0]$  direction of  $1 \times 1$  OH-terminated MgO(111); the ABC stacking sequence of the fcc structure is outlined with an OH group occupying the top (A) surface site. The two available sites for the next Mg layer are the B and C sites, since the A site is already occupied by the OH group (A-A type stackings are energetically highly unfavorable and hence are not discussed further). The energy calculations favor the Mg atom(s) to be at the B site by 0.26 eV/unitcell (i.e., per surface unit cell) compared to the C site. If H is constrained to the A site, when Mg atoms arrive at B—the next available fcc site—H moves upwards to 1.08 Å above the newly formed Mg layer, Fig. 1(a). For convenience we refer to this process as desorption, but it is important to note that the H never leaves the film but remains on the surface. For the new H-Mg-terminated surface, it is not energetically favorable for H to remain on the A site; instead, moving the H to the C site [above the second surface layer of Mg, Fig. 1(b)] lowers the surface energy by 0.55 eV/unit cell. For comparison, having H directly on top of the new Mg layer (site B) raises the surface energy by 0.92 eV/unitcell. These calculations clearly show that the most favorable H site is C, once it is desorbed from O as a result of the new Mg layer formation. The immediate question that arises is: What are the potential barrier(s) and pathways for H to move from the A site (on top of the O sublayer) to the energetically favorable C site? In order to answer this question we calculated the potential energy surface which H would experience moving across the Mg-terminated MgO(111) surface. Figure 1(c) shows the results of these calculations: once the Mg monolayer is formed, the energy barrier of H moving to the C site vanishes, thus H can go freely to its most favorable site [Fig. 1(b) and 1(c)]. The calculated binding energy of H on the C site is rather large, 2.41 eV, and it is 0.55 eV and 1.34 eV larger than that on the A and B sites, respectively. Calculations of  $2 \times 2$  surface cells ( $5.93 \text{ Å} \times 5.93 \text{ Å}$ ) enable partial Mg coverages on the OH-terminated surface to be studied. The results for low coverages ( $\frac{1}{4}$ ) show that the single Mg adsorbs above the H atoms. The H atoms remain coplanar (no change in  $z$ ), but the Mg slightly pushes away the three nearest H atoms. In this configuration the O-H bond is still dominant, and there is no evidence of increased H-H interaction after the Mg adsorption on the surface. As the Mg coverage increases to greater than  $\frac{1}{2}$ , the H atom desorption process discussed previously begins, with no evidence of other mechanisms

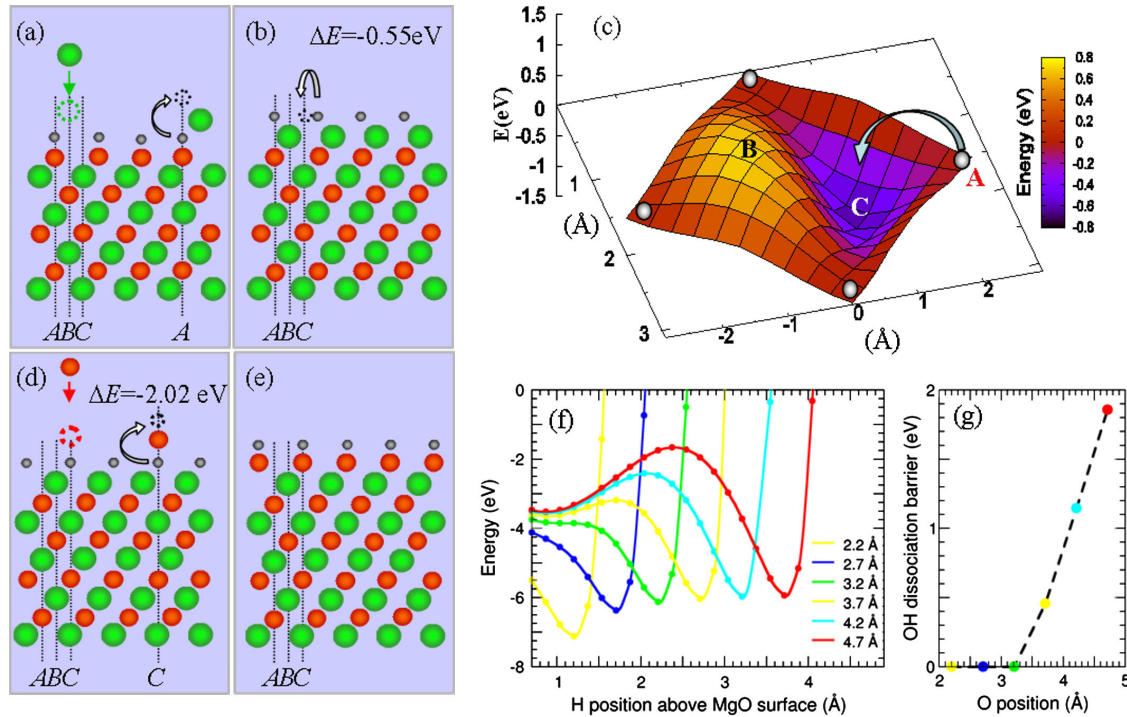


FIG. 1 (color online). Schematics and energetics of H-assisted MgO growth on a MgO(111) surface. The starting surface is OH terminated with O (red [dark grey]) and H (grey) on the A site, and the growth process starts with the addition of a Mg (green [medium grey]) monolayer. As Mg approaches the surface (a), H partially desorbs (the OH bond breaks). This desorption is followed by H moving from site A to site C (b), the site with lowest energy. The 2D potential energy surface for the hydrogen (c), with the energies expressed relative to its starting position, shows that there is no potential barrier for H moving to its most favorable site. The end result of this phase of the growth is a Mg-terminated surface with H as the topmost layer in site C. The growth of the next atomic layer proceeds with O approaching the H on site C (d). There is a large barrier to H desorption which reduces as the O approaches the surface (f) and when O  $\sim 3.2 \text{ \AA}$  the barrier disappears (g), and the OH group forms. The surface energy decreases further with the OH group flip (d). The final surface atomic configuration (e) after a bilayer of growth is identical to the initial surface (a), showing that H acts as a surfactant and enables perfect fcc growth of polar MgO(111) films.

as coverage is increased to  $\frac{3}{4}$  and 1. Thus, the calculations clearly show that H can desorb easily from the O plane once the Mg layer is (mostly) formed, and the newly formed surface configuration preserves the MgO fcc stacking, which is now H(C)-top/ Mg(B)/ O(A)/...

Next, we consider the energetics of O layer formation on this newly formed H-Mg-terminated MgO (111) surface. In order for the film to preserve the fcc structure, the next monolayer of O should occupy the C site, a site where H already sits. In other words the H atoms should desorb once O starts to arrive at the surface. The alternative sites A and B represent stacking fault positions regarding the O adsorption, and their energy is significantly higher compared to that of the C site. To gain insight into the H and O interaction, the potential barrier of H desorption is calculated as O approaches the H in the C site [Figs. 1(f) and 1(g)]. When O is far from the surface the energy barrier is equal to the binding energy of the H atom on the Mg-terminated (111) surface (3.57 eV). As O approaches the surface the barrier decreases [Figs. 1(f) and 1(g)]. At an O distance of 4.7 Å, the barrier height decreases to 1.8 eV, and when O is at 3.2 Å from the surface the barrier vanishes

[Figs. 1(f) and 1(g)], thus the OH molecule can form in the vicinity of the Mg-terminated surface. The OH molecule flips and binds to the Mg-terminated surface by formation of a O-Mg bond [Figs. 1(d) and 1(e)]; the alternative configuration retaining the H-Mg bond and having O as a surface atom is very unstable, with a surface energy 2.02 eV/unit cell higher than the H-O/Mg/... surface. Obviously the minimization of the surface energy is a strong driving force that brings H on top of the O layer, but it is the vanishing or changing of the barriers to H motion as the growth proceeds that is essential; throughout the growth process, H remains strongly bonded to the surface. The surface atomic configuration after adding a bilayer of MgO “growth” is identical to the surface before the onset of the film growth. The presented calculations clearly show that H atoms act as surfactants, which enables the dynamical stabilization of the polar MgO(111) surface. This crucial property of H can facilitate growth of MgO films along the polar [111] direction that is independent of the film thickness, allowing the growth of arbitrarily thick polar MgO(111) films with bulklike fcc structure. It has been shown that polarity can change the properties of the

ultrathin MgO(111) films drastically. Ultrathin films comprising of one to two unit cells ( $\sim 1$  nm in thickness), are predicted to have uncompensated mechanisms as a solution for their polarity, which results from the structural change of the cubic fcc to a nonpolar graphiticlike h-BN(0001) structure [17].

These calculations demonstrate that H provides a “continuous” solution for the polarity of the thin film, stabilizing the growth at the surface dynamically without being incorporated into the film. Such a solution is crucial if we are to achieve controlled growth of polar MgO(111) films. To support this theoretical prediction, we present our experimental work of epitaxial MgO(111) on SiC(0001). MgO films were grown by oxygen-assisted MBE on  $(\sqrt{3} \times \sqrt{3})R30^\circ$  terminated atomically sharp SiC(0001) terraces at  $150^\circ\text{C}$ . A cross section TEM shows a 5 nm thick ( $\sim 40$  atomic layers of MgO) single-crystal

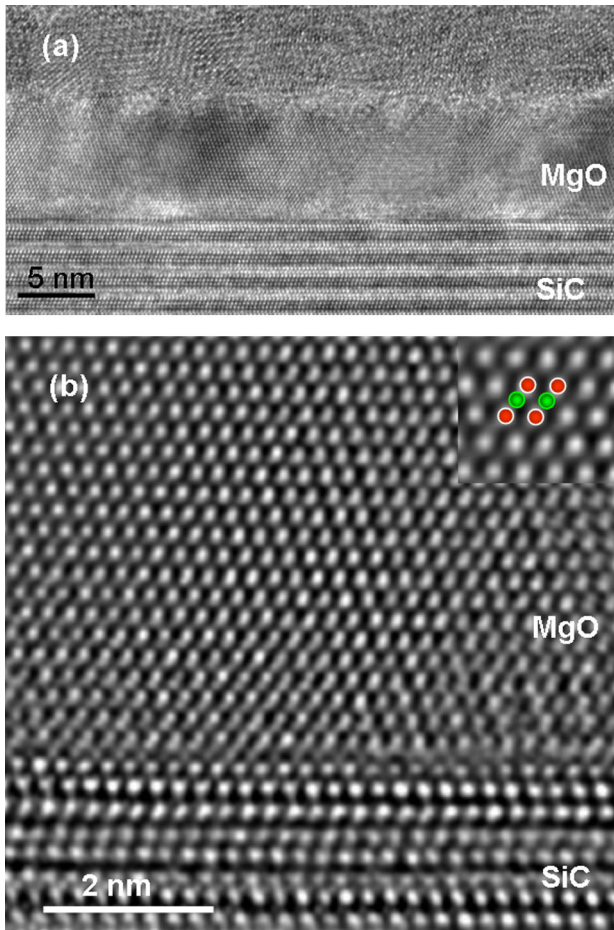


FIG. 2 (color online). HRTEM of MBE grown MgO film on SiC(0001). The film is uniformly grown (a) with no faceting and does not show any presence of stacking faults (b). The film/substrate interface is atomically abrupt and no misfit dislocations are present at the interface (b). Inset in (b) shows the correlation between the image contrast and atomic columns of MgO; white contrast (dots) correspond to O (red [dark grey]), dark contrast to Mg (green [medium grey]).

MgO(111) film (Fig. 2). Digital diffractograms of the high resolution transmission electron microscopy (HRTEM) images give lattice spacings  $d_{111} = 2.97 \text{ \AA}$  and  $d_{002} = 2.08 \text{ \AA}$  for the film. These lattice spacings correspond to those of bulk MgO within the error of the technique. Figure 2 shows an aberration-corrected HRTEM image of the interface and the MgO film. The interface between MgO(111) film and SiC(0001) is atomically abrupt with no dislocations. Image simulations from the MgO film confirm that the white dot contrast in the HRTEM image corresponds to the Mg atomic columns, while the dark contrast corresponds to O columns (inset, Fig. 2). The TEM data confirm growth of a fully fcc-ordered epitaxial single-crystal polar MgO(111) film with the following crystallographic relation:  $\text{MgO}(111) \parallel \text{SiC}(0001)$  and  $\text{MgO}(11-2) \parallel \text{SiC}(1-100)$ .

The final question we address is: Is H really involved in the growth process, as our calculations show? Even though H cannot be detected directly, the presence of surface H when bonded to O gives a unique feature in the surface O 1s peak, a shoulder shift of  $\sim 2.0$  eV [9,18], which can be detected by x-ray photoelectron spectroscopy (XPS). This feature has been shown to be a fingerprint of H-stabilized polar surfaces (9). Figure 3 presents an XPS spectrum from the MgO(111) film around the O 1s peak. A shoulder feature due to the O-H bond is clearly seen on the left-hand side of the O 1s peak confirming that the MgO(111) film surface is H terminated, which is in good agreement with the modeling results presented above. H remains on the surface due to its surfactant properties, and provides a continuous real-time stabilization mechanism for the MgO(111) surface polarity. In other words, H alleviates the problem that arises from the divergent nature of the electrostatic potential for thin polar films.

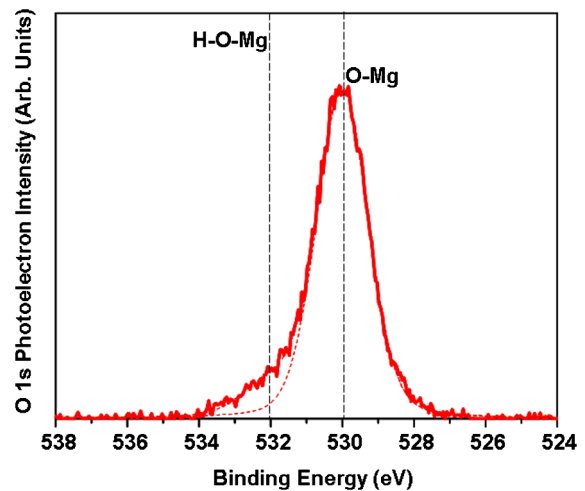


FIG. 3 (color online). *In situ* XPS from the MBE grown MgO(111) film. The shoulder of the O 1s peak shows that the film is OH terminated.

In summary, we have shown that H can play the role of surfactant in the growth of polar oxide films. Our calculations demonstrate that H is not static during the growth, and we have shown how the position of the H atoms, the barriers, and the pathways change. The surfactant property of H provides a dynamical solution to the fundamental problem in the growth of polar oxide films arising from the large polar oxide surface energy, by effectively screening the surface dipole moment and thus lowering the MgO(111) surface energy. Controlled growth of polar MgO(111) provides opportunities to create new types of interface structures that could expand the use of MgO in tunnel barriers, diffusion barriers, template oxides, as a dielectric, and to interface-engineer artificial polar oxide structures in the quest to tailor the functional properties, as already demonstrated on perovskite polar oxide multilayer structures [19]. Finally, the surfactant properties of H should enable the controlled growth of other strongly polar oxide films, thus opening the way for creating novel polar oxide artificial multilayered structures.

Work at UWM was supported by the U.S. Department of Energy, Office of Basic Energy Sciences (DE-FG02-06ER46328). V. K. L. would like to acknowledge the support from RAEng/EPSCRC fellowship.

\*Corresponding author

vlado.lazarov@york.ac.uk

- [1] C. Noguera, *J. Phys. Condens. Matter* **12**, R367 (2000).
- [2] J. Goniakowski, F. Finocchi, and C. Noguera, *Rep. Prog. Phys.* **71**, 016501 (2008).
- [3] V. E. Henrich, P. A. Cox, *The Surface Science of Metal Oxides* (Cambridge University Press, Cambridge, 1994).
- [4] O. Maksimov *et al.*, *J. Cryst. Growth* **310**, 2760 (2008).
- [5] M. Kiguchi *et al.*, *Phys. Rev. B* **68**, 115402 (2003).
- [6] T. L. Goodrich *et al.*, *Appl. Phys. Lett.* **90**, 042910 (2007).
- [7] K. Matsuzuki, H. Hosono, and T. Susaki, *Phys. Rev. B* **82**, 033408 (2010).
- [8] B. Warot *et al.*, *Appl. Surf. Sci.* **188**, 151 (2002).
- [9] V. K. Lazarov *et al.*, *Phys. Rev. B* **71**, 115434 (2005).
- [10] H. C. Poon *et al.*, *Surf. Sci.* **600**, 2505 (2006).
- [11] K. Refson *et al.*, *Phys. Rev. B* **52**, 10 823 (1995).
- [12] R. Plass *et al.*, *Phys. Rev. Lett.* **81**, 4891 (1998).
- [13] J. Ciston, A. Subramanian, and L. D. Marks, *Phys. Rev. B* **79**, 085421 (2009).
- [14] E. Wimmer *et al.*, *Phys. Rev. B* **24**, 864 (1981).
- [15] M. Weinert *et al.*, *Phys. Rev. B* **26**, 4571 (1982).
- [16] S. Clark *et al.*, *Z. Kristallogr.* **220**, 567 (2005).
- [17] J. Goniakowski, C. Noguera, and L. Giordano, *Phys. Rev. Lett.* **98**, 205701 (2007).
- [18] S. A. Chambers *et al.*, *Science* **297**, 827 (2002).
- [19] A. Ohtomo, H. Y Hwang, *Nature (London)* **427**, 423 (2004).